Nylon-6/rubber blends

Part III *Stresses in and around rubber particles and cavities in a nylon matrix*

K. DIJKSTRA*, G. H. TEN BOLSCHER
University of Twente, P.O. Box 217, 7500 AE Enschede, The Netherlands

The stress field around a rubber particle and a cavitated particle in a nylon/rubber blend has been studied using an analytical and a finite element approach. Attention was paid to the influence of the mechanical properties of the dispersed phase and the applied stress state. The results show that the choice of the bulk modulus of the elastomer is crucial. It appeared that especially with a triaxial stress, the Von Mises stress increased strongly upon cavitation (a more than five-fold increase close to the particle) while the hydrostatic stress only increased slightly. Also, the stresses in particles in the neighbourhood of a cavity have been calculated. Stresses in particles lying in or close to the equatorial plane of the cavity were higher than stresses in the other particles. Therefore, propagation of cavitation is most likely to occur perpendicular to the applied stress.

1. Introduction

When blending a soft elastomeric material into a rigid nylon matrix, it is expected that the mechanics of the resulting system will differ from that of the pure nylon. Because the onset of deformation processes such as shearbanding or crazing is dependent on the internal stresses, it is necessary to understand the way in which the second phase affects the mechanics of the blend. The stress state (uniaxial, as in a tensile test, or highly triaxial which will be the case ahead of a notch), the properties of the rubber and the morphology may all be important.

Calculations have been made concerning the stress field around a rubber particle in a nylon matrix. Because it is now generally believed that cavitation of the rubber phase is a necessary step in the fracture process of nylon/rubber blends [1–5], the influence of cavitation on the internal stresses has also been calculated. The first part of this paper concerns blends with a low rubber content, so that particles can be considered to be isolated inclusions. The stress field around an inclusion was calculated analytically as a function of rubber properties and applied stress state.

In the second part, predictions are made of the interaction of stress fields of neighbouring particles at higher volume fractions of impact modifier. Because it has not been possible to derive an analytical solution for these multi-particle systems, a finite element analysis has been used to calculate the stresses and displacements around the particles. Also in this part, attention is paid to the influence of the mechanical properties of the rubber and the applied stress state.

2. Stresses in and around an isolated elastic inclusion

The solutions of the stress and displacement field around a spherical or cylindrical elastic inclusion in an elastic matrix, subjected to a uniform uniaxial tensile stress far way from the inclusion, were obtained by Goodier in 1933 [6]. Following his analysis, the stresses and displacements in and around a rubber inclusion subjected to a given biaxial stress far away from the inclusion are calculated.

Consider an infinite cylindrical inclusion in an elastic matrix under plane strain conditions (see Fig. 1). Goodier gives the following set of equations for the stress and displacement concentration in and around the inclusion (Equation 1). The elastic constants in Equation 1 are distinguished by subscript 1 for the matrix and subscript 2 for the inclusion.

Outside the inclusion $(r \geqslant a)$

$$u_{r1} = \frac{A}{r} + \left[-\frac{B}{r^3} + \frac{2C}{r}(1 - \nu_1) \right]\cos 2\theta$$

$$u_{\theta 1} = -\left[\frac{B}{r^3} + \frac{C}{r}(1 - 2\nu_1) \right]\sin 2\theta$$

$$\sigma_{rr1} = 2G_1\left[\frac{A}{r^2} + \left(\frac{3B}{r^4} - \frac{2C}{r^2} \right)\cos 2\theta \right]$$

$$\sigma_{\theta\theta 1} = 2G_1\left[\frac{A}{r^2} - \frac{3B}{r^4}\cos 2\theta \right]$$

$$\sigma_{r\theta 1} = 2G_1\left[\frac{3B}{r^4} - \frac{C}{r^2} \right]\sin 2\theta$$

(1a)
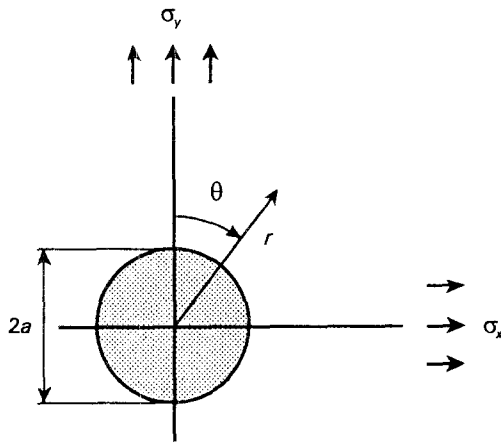
Figure 1 A cylindrical inclusion in an infinite elastic matrix subjected to a biaxial stress.

$$\frac{A}{a^2} = \frac{\sigma_y + \sigma_x}{4G_1} \cdot \left[\frac{(1 - 2v_2)G_1 - (1 - 2v_1)G_2}{(1 - 2v_2)G_1 + G_2}\right] \Bigg\rangle$$

$$\frac{B}{a^4} = \frac{\sigma_y - \sigma_x}{4G_1} \cdot \left[\frac{G_1 - G_2}{G_1 + (3 - 4v_1)G_2}\right]$$

$$\frac{C}{a^2} = \frac{\sigma_y - \sigma_x}{2G_1} \cdot \left[\frac{G_1 - G_2}{G_1 + (3 - 4v_1)G_2}\right]$$

$$F = \frac{(\sigma_y + \sigma_x)(1 - v_1)(1 - 2v_2)}{2[(1 - 2v_2)G_1 + G_2]}$$ (3)

$$G = \frac{(\sigma_y - \sigma_x)(1 - v_1)}{G_1 + (3 - 4v_1)G_2}$$

$$H = 0$$

Inside the inclusion $(r \leq a)$

$$u_{r2} = Fr + (Gr + 2v_2Hr^3)\cos2\theta \Bigg\rangle$$

$$u_{\theta2} = -[Gr + (3 - 2v_2)Hr^3]\sin2\theta$$

$$\sigma_{rr2} = 2G_2\left[\frac{F}{1 - 2v_2} + G\cos2\theta\right]$$ (1b)

$$\sigma_{\theta\theta2} = 2G_2\left[\frac{F}{1 - 2v_2} - (G + 6Hr^2)\cos2\theta\right]$$

$$\sigma_{r\theta2} = -2G_2(G + 3Hr^2)\sin2\theta$$

A uniform biaxial stress in an undisturbed system gives the following displacements and stresses (Equation 2).

$$u_{r\infty} = \frac{r}{4G_1}[(\sigma_y + \sigma_x)(1 - 2v_1) \Bigg\rangle$$

$$+ (\sigma_y - \sigma_x)\cos2\theta]$$

$$u_{\theta\infty} = -\frac{r}{4G_1}(\sigma_y - \sigma_x)\sin2\theta$$

$$\sigma_{rr\infty} = \frac{1}{2}(\sigma_y + \sigma_x) + \frac{1}{2}(\sigma_y - \sigma_x)\cos2\theta$$ (2)

$$\sigma_{\theta\theta\infty} = \frac{1}{2}(\sigma_y + \sigma_x) - \frac{1}{2}(\sigma_y - \sigma_x)\cos2\theta$$

$$\sigma_{r\theta\infty} = -\frac{1}{2}(\sigma_y - \sigma_x)\sin2\theta$$

When the stresses and displacements at the boundary $(r = a)$ are equated, the constants A, B, C for the matrix and F, G, H for the dispersed phase can be calculated. The resulting constants are given in Equation 3. When the stress in the x-direction is set to zero, the solution reduces to the one given by Goodier. It is possible now to calculate the stresses in the complete system when the elastic constants of matrix and inclusion and the stress state far away from the inclusion are known. Inherent in the solutions is that they are only valid for isolated inclusions, i.e. for low volume fractions of the dispersed phase. At high volume fractions of the dispersed phase interaction between stress fields of neighbouring particles will make it impossible to use this kind of analysis.

When calculations of this kind are carried out, it appears that due to the high Poisson's ratio of the elastomer (v_2 is close to 0,5), also under uniaxial loading the stress state inside the inclusion is almost perfectly hydrostatic. Therefore, the bulk modulus of the rubber will control the stresses inside the inclusion and consequently the stress concentration in the matrix. This is demonstrated in Fig. 2 where the hydrostatic stress (the first invariant of the stress tensor) is plotted versus the bulk modulus of the rubber. Varying the shear modulus over two decades from 1–100 MPa (typical values for the rubbers used) while keeping the bulk modulus constant, has no effect on the magnitude of the internal stresses in the inclusion. Only when the shear modulus of the inclusion is close to the shear modulus of the matrix is a minor decrease in the hydrostatic tension observed.

When calculating the bulk modulus from the Young's modulus and the Poisson's ratio, the calculated bulk modulus will be very sensitive to the Poisson's ratio when the latter is close to 0.5. It was demonstrated by Narisawa *et al.* [7] that the stress concentration around a particle was strongly dependent on the Poisson's ratio in that region.

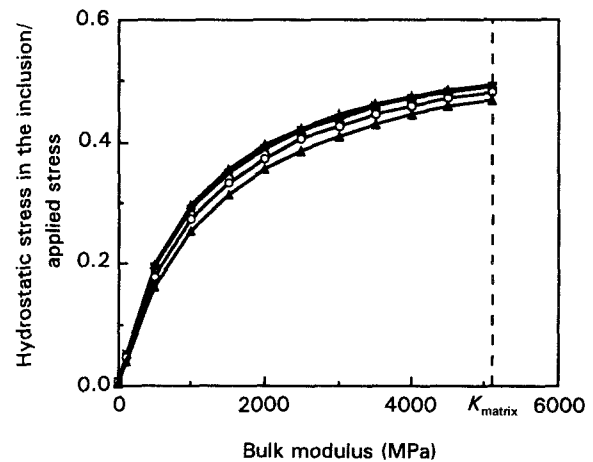It is general knowledge that the bulk moduli for most polymers are of the same order of magnitude,

Figure 2 Hydrostatic stress in the inclusion subjected to a uniaxial stress divided by the applied remote stress versus the bulk modulus of the dispersed phase for different shear moduli of the dispersed phase: G_2 (MPa): (△) 1, (+) 10, (×) 100, (○) 500, (▲) 1000. Matrix properties are $E_1 = 2.82$ GPa, $v_1 = 0.41$. $K_1 = 5100$ MPa.

despite the fact that the Young's moduli can vary over some decades. Van Krevelen [8] gives values between 2.0 GPa (natural rubber) and 7.4 GPa (phenol form-aldehyde resin). For nylon-6, a value is reported of 5.1 GPa. The bulk modulus of most elastomers is a little lower (between 2.0 and 3.5 GPa) [8]. Therefore, in all the calculations presented here (the analytical as well as the numerical calculations), the bulk modulus is chosen according to reported values in the literature and the Poisson's ratio is calculated from the shear modulus and the bulk modulus.

When the hydrostatic and the Von Mises stress in inclusion and matrix are plotted (Fig. 3) for two very different types of impact modifiers (an LDPE and a poly(butadiene)-like material) it is clear that the external stress field is more or less the same for both materials. Although there is a tendency that the stresses around a very soft inclusion are somewhat higher (especially the Von Mises stress) than those around a stiffer particle, these differences are too small to

explain the observed large differences in impact behaviour [3, 9].

In Fig. 4, the influence of cavitation on the hydrostatic and the Von Mises stress are given. In both cases, the hydrostatic stress does not change upon cavitation in the equatorial plane. Under a uniaxial load, there is a moderate increase in the Von Mises stress after cavitation. However, under a biaxial load there is a more than five-fold increase in the Von Mises stress around the particle after cavitation. This indicates that indeed cavitation is necessary for large scale yielding ahead of a notch or a running crack.

So far, only data have been presented of stresses in the equatorial plane. In Fig. 5, the hydrostatic stress and the Von Mises stress around the particle are given as a function of the angle θ. The Von Mises stress shows maxima at the equator and at the pole. Before cavitation, the maximum at the equator is slightly higher than that at the pole. However, after cavitation yielding will preferentially start at the equator of the inclusion.
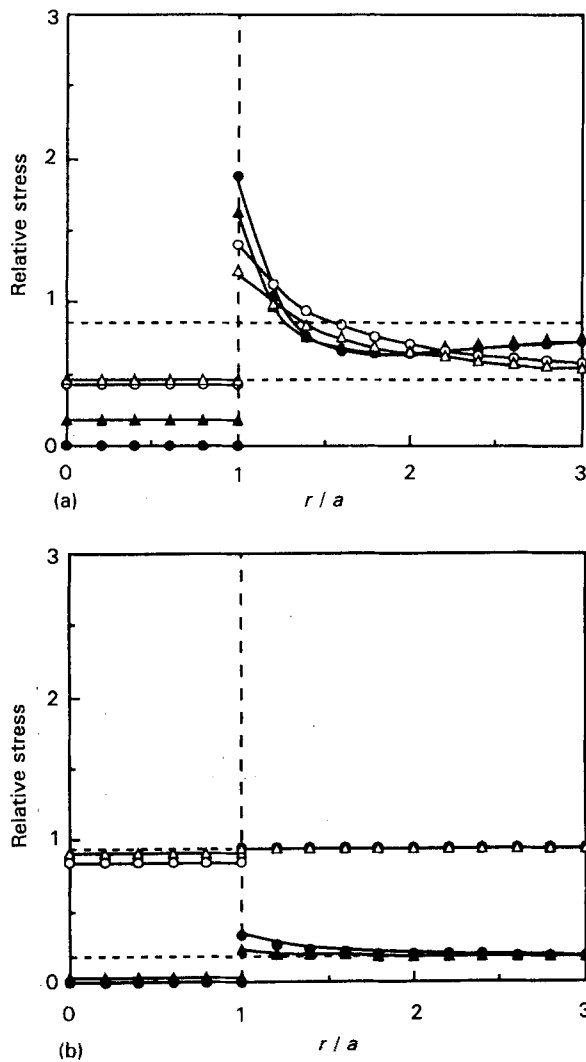

Figure 3 Stresses in the equatorial plane ($\theta = \pi/2$) relative to σ_y for different rubber properties: BR, $G_2 = 1$ MPa, $K_2 = 2500$ MPa, (●) Von Mises stress, (○) hydrostatic stress; LDPE, $G_2 = 100$ MPa, $K_2 = 3500$ MPa, (▲) Von Mises stress, (△) hydrostatic stress. (- - -) Stresses in the undisturbed geometry. Elastic constants of the matrix: $G_1 = 1000$ MPa, $K_1 = 5100$ MPa. (a) Uniaxial tension ($\sigma_x = 0$). (b) biaxial tension ($\sigma_x = \sigma_y$).
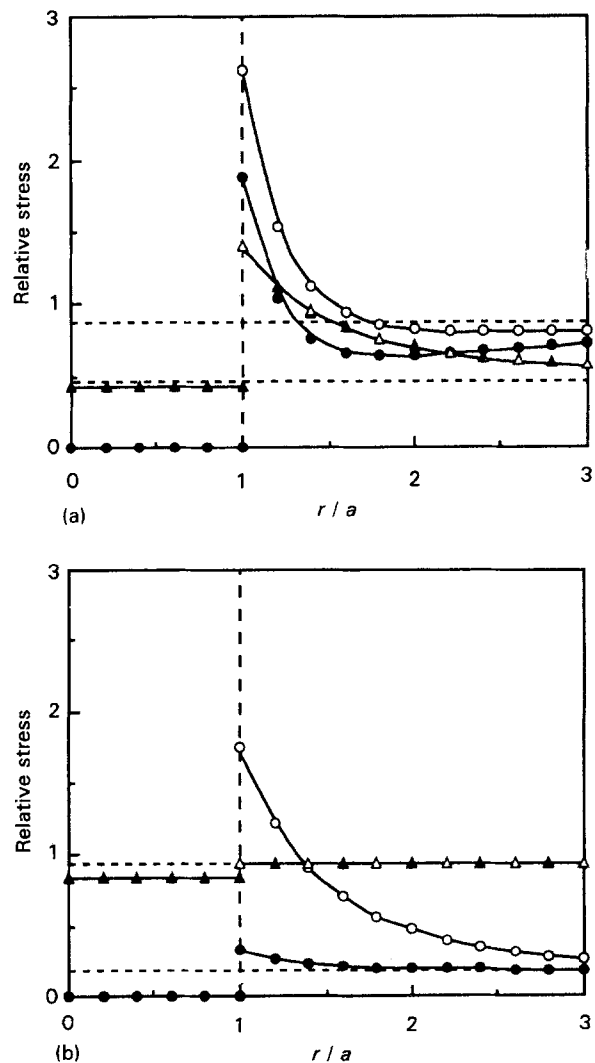
Figure 4 Stresses in the equatorial plane ($\theta = \pi/2$) relative to σ_y (●, ▲) before and (○, △) after cavitation: (●, ○) Von Mises stress, (▲, △) hydrostatic stress. (- - -) Stresses in the undisturbed geometry. Elastic constants used: matrix $G_1 = 1000$ MPa, $K_1 = 5100$ MPa; inclusion $G_2 = 1$ MPa, $K_2 = 2500$ MPa. (a) Uniaxial tension ($\sigma_x = 0$), (b) biaxial tension ($\sigma_x = \sigma_y$).
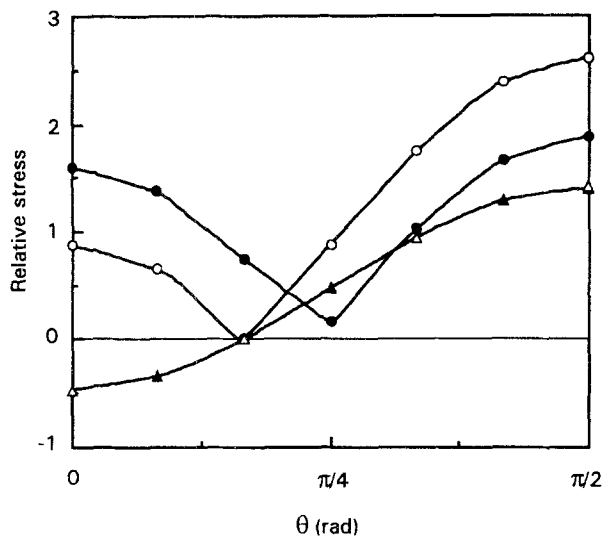
Figure 5 Stresses around a uniaxially loaded inclusion $(r/a = 1)$ relative to σ_y ($\bullet$, $\blacktriangle$) before and ($\bigcirc$, $\triangle$) after cavitation: ($\bullet$, $\bigcirc$) Von Mises stress; ($\bullet$) before cavitation, ($\bigcirc$) after cavitation; hydrostatic stress: ($\blacktriangle$) before cavitation, ($\triangle$) after cavitation. Elastic constants used: matrix $G_1 = 1000$ MPa, $K_1 = 5100$ MPa; inclusion $G_2 = 1$ MPa, $K_2 = 2500$ MPa.

It is well known that the stresses at the pole of a soft inclusion are compressive. This is demonstrated in Fig. 5 by the negative hydrostatic stress at $\theta = 0$. Surprisingly, the hydrostatic stress does not change upon cavitation. Apparently, a change in the radial stress is accompanied by an equal but opposite change in the tangential stress.

3. Stress distribution in multiple particle systems

With higher rubber contents, stress fields around neighbouring particles start to overlap. An often used criterion for stress-field overlap is that the distance between particles should be smaller than the diameter of the particles. This means that the rubber volume fraction should be larger than 0.085. Because most commercial toughened nylons have a rubber volume fraction between 0.15 and 0.30, it is evident that interaction between stress fields will take place in these materials. Therefore, the stress and strain distribution no longer can be calculated analytically and has to be approximated using a finite element analysis.

When modelling a two-phase system such as a nylon/rubber blend, a number of problems is encountered. The first problem is that it will not be possible to model a blend with a large number of randomly distributed particles. Therefore, the particles are normally thought to be arranged in a regular way (e.g. a cubic array, a BCC stacking, etc.). Using the symmetry in particle arrangement, multi-particle systems can then be modelled with only one or a few particles. The disadvantage of the approximation using a regular distribution is the concentration of rubber in layers in this model. The effective matrix surface in these layers will be smaller than when calculated using a random distribution [10]. Therefore, the calculated stresses in these layers will be too high.

Another problem is that the computers and software normally available are not powerful enough to handle a complex three-dimensional analysis. If the system is symmetrical about an axis, this symmetry can be used to reduce the three-dimensional system to a two-dimensional system without loss of accuracy. When this is not the case, the stresses and strains can be calculated in a two-dimensional system by assuming plane stress or plane strain, though the solutions derived from these models are not necessarily representative for the system.

In the literature, solutions of both types are found. Guild and Young [11] modelled an epoxy/rubber system under a uniaxial load with an axial-symmetric FEM model and varying rubber contents. They indeed found a significant overlap of stress fields with an interparticle distance smaller than the particle size. Their calculations only showed a small increase in stress concentration after cavitation, which led to the conclusion that a rubber particle is, from a mechanical viewpoint, identical to a void. The rubber properties they used in their model, though, had a bulk modulus of about a factor of 30 below realistic values. Because in the previous paragraph it was concluded that in a two-dimensional plane-strain system cavitation leads, also with uniaxial loading, to a significant increase in the Von Mises stress, the analytical solution of Goodier for a two-dimensional system with axial symmetry is compared in Fig. 6 with the two-dimension plane-strain solution using the rubber properties of Guild and Young. In this figure the solutions are also given for a nylon/rubber blend using a rubber with the same Young's modulus as the rubber used by Guild and Young but now with a more realistic bulk modulus of 2000 MPa. It is clear that the material with the low bulk modulus is in both cases, identical to a void. When the bulk modulus is set to a correct value, and also when using the axial symmetry, cavitation does not exert much influence on the Von Mises stress in the matrix. For the plane strain model, however, there now is a significant increase in the Von Mises stress. This can be explained by the fact that the stresses in the plane-strain situation are more triaxial than those in the axially symmetric case and that, therefore, the rubber phase will carry a higher stress. It can be expected that under biaxial loading these differences between the two types of solutions are much smaller because then in both cases the stress state is highly triaxial.

Fukui *et al.* [12] used a simplified two-dimensional plane-strain model with five particles arranged in a cubic array, loaded under an angle of 45° to the cell axis. A similar, but more accurate, model was employed by Huang and Kinloch [13]. The bulk modulus of the dispersed phase used in both studies (165 and 33.3 MPa, respectively) was too low to expect a significant difference between a voided and a rubber-filled system. Also, the models were loaded uniaxially, so the authors concluded that, despite the plane-strain condition, cavitation was not necessary for large-scale matrix yielding. Fukui *et al.* as well as Huang and Kinloch, also performed a plastic analysis and both sets of authors found that shear bands developed
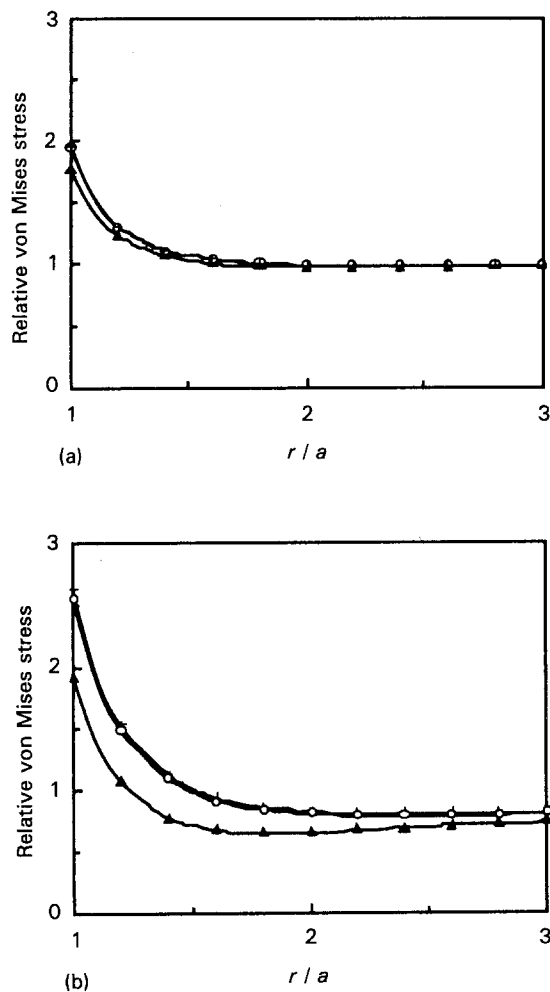
Figure 6 Von Mises stress in the equatorial plane ($\theta = \pi/2$) for two-dimensional approximations of the three-dimensional system of a rubber particle in a nylon matrix. (+) Void, ($\bigcirc$) $E_2 = 0.4$ MPa, $K_2 = 66.7$ MPa ($v_2 = 0.499$, rubber properties used by Guild and Young), ($\blacktriangle$) $E_2 = 0.4$ MPa, $K_2 = 2000$ MPa ($v_2 = 0.49997$, as before, but with a corrected bulk modulus). (a) Two-dimensional-axial symmetric system, (b) two-dimensional plane-strain system.

under an angle of 45° to the main principal stress. This may be caused by the fact that this was also the direction where the nearest particle was situated.

A number of questions still remain unanswered. First of all, the studies reported in the literature concerning particle-filled systems only present solutions of systems subjected to a uniaxial load. However, for a better understanding of rubber toughening of polymers, it is more relevant to look at systems subjected to a stress state as being present ahead of a notch or crack tip, which is highly triaxial.

Another point of interest is the way in which the cavitation zones develop. All the calculations found in the literature compare the rubber-filled system with a completely cavitated system. Micrographs of deformed blends [9, 14] have shown that in stressed blends, rows of cavitated particles are formed normal to the main principal stress. This suggests that cavitation of one particle affects the stresses in the surrounding particles in such a way that cavitation occurs preferentially in the particle lying in the equatorial plane of the cavitated particle.

3.1. The finite element model

The calculations were performed on a VAX micro-computer. The software used for the finite element calculations was ANSYS. The matrix and the dispersed phase were modelled with a eight-node isoparametric solid two-dimensional element with two degrees of freedom (displacement in the x- and y-direction). For the third dimension, plane-strain behaviour was assumed. Linear elastic behaviour was assumed for both the matrix and the rubber. Owing to restrictions of the software used, the number of elements for all models was limited to 500.

Most calculations were performed on a model with five particles in a BCC packing. In Fig. 7 the element model is given. In the case of a BCC packing, the relation between interparticle distance, ID, rubber particle size, d, and rubber volume fraction, φ_r, is slightly different from the relation (for a cubic array) given by Wu [15] and is now given by Equation 4. Choosing the rubber volume fraction gives the ratio between interparticle distance and particle size in the FEM model, given in Fig. 7.

$$ID = d\left[\frac{1}{2}3^{1/2}\left(\frac{\pi}{3\varphi_r}\right)^{1/3} - 1\right] \qquad (4)$$

In the FEM model, the displacement in the x-direction of the left boundary and the displacement in the y-direction of the lower boundary is fixed. The upper boundary of the model is given a uniform displacement in the y-direction. The displacements in the x-direction of the nodes on the right boundary of the model are coupled. The stress state ahead of the crack tip is highly triaxial. This stress state is simulated by setting the displacements in the x-direction of the right boundary to zero.

The model represented in Fig. 7 has a ratio between interparticle distance and particle size corresponding to a rubber content of 25 vol %. A similar model was generated with a ratio between ID and d corresponding to a rubber content of 5 vol %. The dotted elements are modelled with the elastic properties of the rubber.

The calculations were done with the following elastic constants for the matrix: $G = 1000$ MPa, $K = 5100$ MPa. For the rubber, two different sets of constants were used: one poly(butadiene)-like material with $G = 1$ MPa and $K = 2500$ MPa and an LDPE-like material with $G = 100$ MPa and $K = 3500$ MPa.

The system was also evaluated with five holes and with four particles and a void at the position of particle 1. The applied displacement was in all cases the same.

3.2. Results and discussion

In Figs 8 and 9, the results are given of the FEM calculation on the five-particle model with the poly-butadiene-type material as impact modifier. The numerical solution for the low rubber volume fraction is very similar to the analytical solution under similar loading conditions. When the two different rubber contents are compared, the effect of overlap of stress
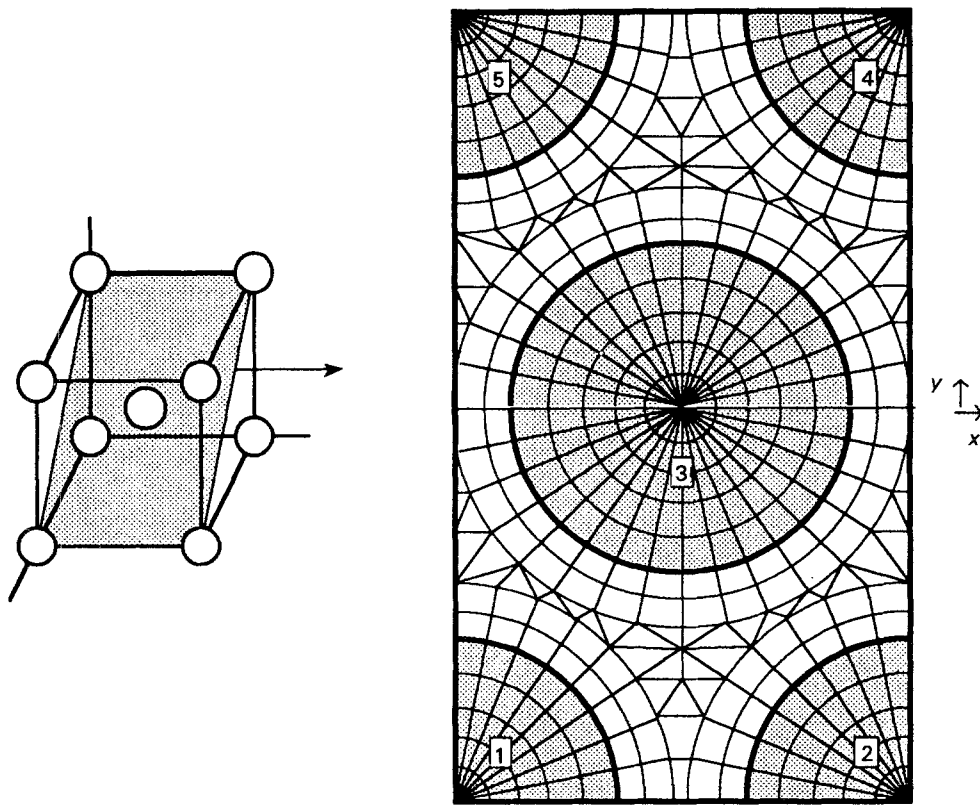
4290

Figure 7 FEM model of five spherical particles in a BCC packing. The ratio ID/d corresponds to a rubber volume fraction of 0.25.
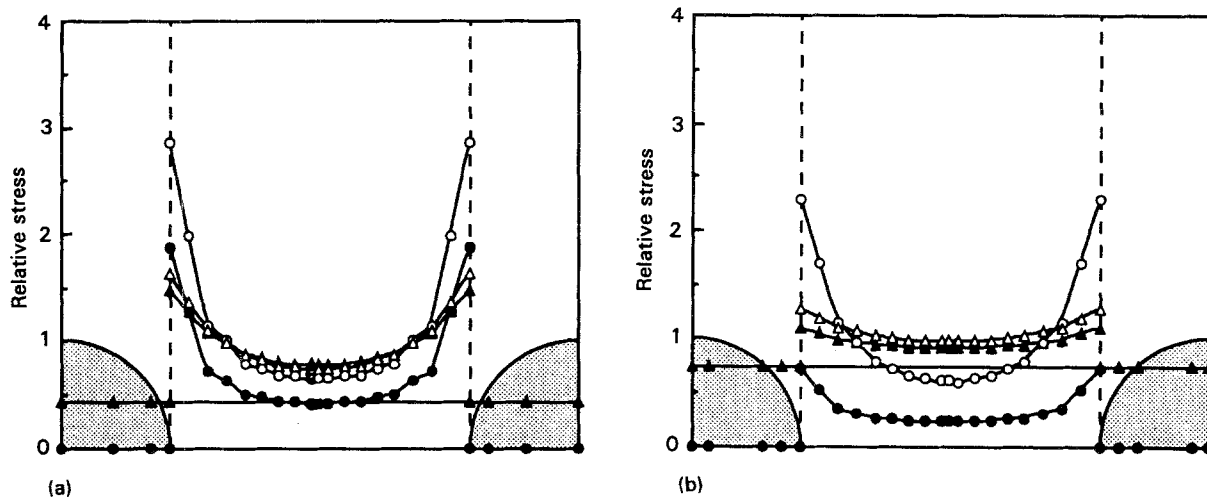

(a)   (b)

Figure 8 The Von Mises stress and the hydrostatic stress over the lower boundary of the model, relative to the average applied stress on the upper boundary, (●, ▲) before and (○, △) after complete cavitation for two different loading conditions: (●, ○) Von Mises stress; (▲, △) hydrostatic stress. Rubber content 5 vol %, rubber properties $G_2 = 1$ MPa, $K_2 = 2500$ MPa. (a) Right boundary of the model is free to contract, (b) right boundary of the model is fixed.

fields is clearly visible. In all cases the stresses in the matrix are considerably higher when the rubber content is high.

Also, when the right boundary is free to contract, cavitation results in a significant rise in the Von Mises stress. As mentioned before, this is caused by the two-dimensional plane-strain approximation and this will not be the case when the system is calculated using a more realistic two-dimensional axial-symmetric model. When the right boundary is fixed, there is a strong increase in the Von Mises stress, especially when the rubber/void concentration is high.

The hydrostatic stress in the ligament does not change much after cavitation when the rubber concentration is low. For the high rubber content, though, there is a distinct rise in the hydrostatic stress when the rubber cavitates.

When the dispersed phase is modelled with the LDPE-like material parameters, the solutions obtained are very similar to those presented in Figs 8 and 9. This is in agreement with the analytical solutions presented in Fig. 3.

In order to investigate whether cavitation of one particle causes a preferred growth of cavities in a plane
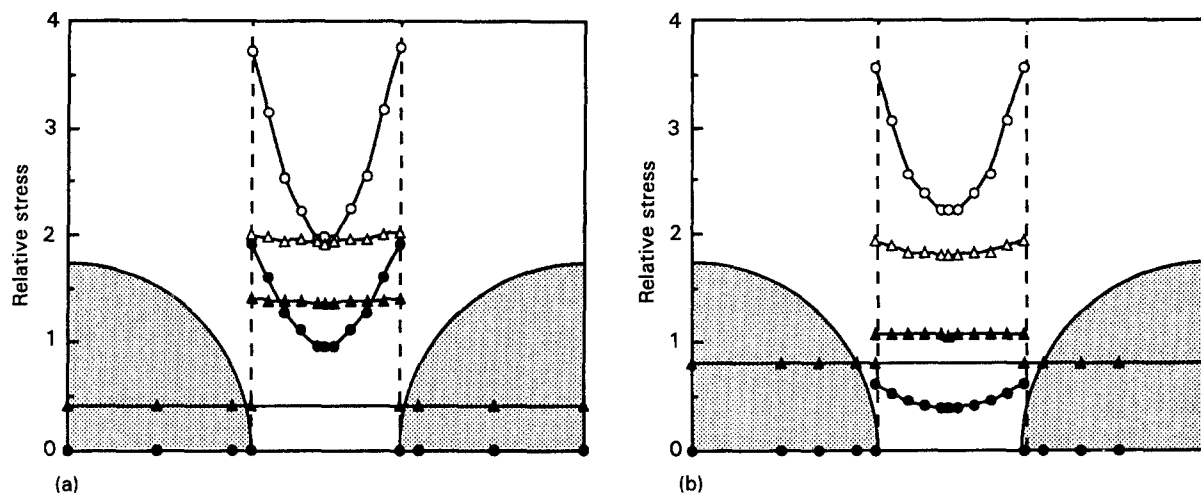
4291

Figure 9 The Von Mises stress and the hydrostatic stress over the lower boundary of the model, relative to the average applied stress on the upper boundary, (●, ▲) before and (○, △) after complete cavitation for two different loading conditions: (●, ○) Von Mises stress; (▲, △) hydrostatic stress. Rubber content 25 vol %, rubber properties $G_2 = 1$ MPa, $K_2 = 2500$ MPa. (a) Right boundary of the model is free to contract, (b) right boundary of the model is fixed.
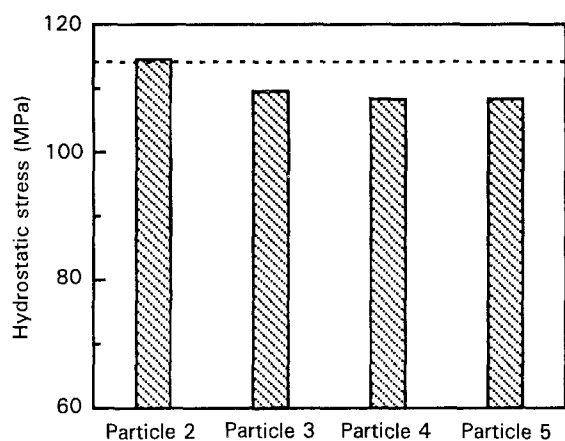

Figure 10 Hydrostatic tension in particles 2–5 after cavitation of particle 1. (- - -) The hydrostatic stress in the particles before cavitation. The right boundary of the model is fixed. See, for particle numbering, Fig. 7 (rubber volume fraction is 0.25).

perpendicular to the main principal stress, the hydrostatic stress in particles 2–5 is calculated before and after cavitation of particle 1 with an equal applied displacement of the upper boundary of the model. The results are given in Fig. 10, where it can be seen that cavitation of particle 1 causes a decrease in hydrostatic stress in all the particles except for the particle lying in the equatorial plane of the void (particle 2), where a slight increase of hydrostatic stress is observed. From this it can be concluded that indeed cavitation takes place preferentially in a plane perpendicular to the main principal stress. The observed effects are, however, small and probably only important when cavitation is critical.

When a cavitated zone of some length is formed, the appearance will be quite similar to that of a craze, only on a different scale. Thus, the growth of these cavitated bands can probably be described in a similar way as craze growth, with a maximum in the stress concentration on the edge of the cavitated zone.

4. Conclusions

Because of the high Poisson's ratio of the dispersed phase, the stress state in the rubber will be almost perfectly hydrostatic and the height of the hydrostatic stress is controlled by the bulk modulus. Owing to the fact that the bulk modulus of the rubber phase is of the same order of magnitude as that of the matrix, the rubber will, despite the low Young's modulus, carry an appreciable part of the load. That is why a correct choice of the bulk modulus is essential.

From the literature and our own calculations it follows that under a uniaxial load, cavitation is not necessary for yielding, because the Von Mises stress in the matrix, compared to the applied stress, does not change significantly upon cavitation. Also, the hydrostatic stress is rather independent of the mechanical properties of the dispersed phase. Modelling the rubber with a Young's modulus from very low to relatively high values gives similar results.

However, when the stress state ahead of the notch or crack tip is simulated, there is a strong increase in the Von Mises stress when the rubber particles are replaced by voids while the differences between different types of rubber are still small. This means that indeed cavitation is necessary for the formation of a large plastic zone ahead of a running crack. Different impact behaviour of blends with different types of rubber and the same morphology cannot be explained from differences in the stress field around the rubber particles.

Cavitation of a particle under constant applied strain tends to decrease the hydrostatic stress of the surrounding particles, except for the particles in or close to the plane perpendicular to the main principal stress, where a small rise in hydrostatic stress is observed. Therefore, cavitation zones grow in a similar way to crazes or cracks.

Acknowledgements

References

1. F. RAMSTEINER and W. HECKMANN, *Polym. Commun.* **26** (1985) 199.
2. R. J. M. BORGGREVE, R. J. GAYMANS, J. SCHUIJER and J. F. INGEN HOUSZ, *Polymer* **28** (1987) 1489.
3. R. J. M. BORGGREVE, R. J. GAYMANS and J. SCHUI-JER, *ibid.* **30** (1989) 71.
4. R. J. M. BORGGREVE, R. J. GAYMANS and H. M. EICHENWALD, *ibid.* **30** (1989) 78.
5. F. SPERONI, E. CASTOLDI, P. FABBRI and T. CASI-RAGHI, *J. Mater. Sci.* **24** (1989) 2165.
6. J. N. GOODIER, *ASME Appl. Mech. Trans.* **55** (1933) 39.
7. I. NARISAWA. T. KURIYAMA and K. OJIMA, *Makromol. Chem. Makromol. Symp.* **41** (1991) 87.
8. D. W. VAN KREVELEN, in "Properties of Polymers" edited by D. W. van Krevelen (Elsevier Scientific, Amsterdam 1976) p. 271.
9. K. DIJKSTRA, A. J. OOSTENBRINK, R. J. GAYMANS, "8th International Conference on Deformation, Yield and Fracture of Polymers," PRI Conference, Cambridge, April 1991, paper 9.
10. K. DIJKSTRA, A. VAN DER WAL and R. J. GAYMANS, *J. Mater. Sci.* in press.
11. F. J. GUILD and R. J. YOUNG, *ibid.* **24** (1989) 2454.
12. T. FUKUI, Y. KIKUCHI and T. INOUE, *Polymer* **32** (1991) 2367.
13. Y. HUANG and A. J. KINLOCH, *J. Mater. Sci.* **27** (1992) 2753.
14. H. J. SUE, "8th International Conference on Deformation, Yield and Fracture of Polymers," PRI conference Cambridge, April 1991, paper 63.
15. S. WU, *Polymer* **26** (1985) 1855.